

Rectification in single molecular dimers with strong polaron effect

Gregers A. Kaat and Karsten Flensberg

Nano-Science Center, Niels Bohr Institute, Universitetsparken 5, 2100 Copenhagen, Denmark

(Received 6 November 2004; revised manuscript received 18 January 2005; published 14 April 2005)

We study theoretically the transport properties of a molecular two-level system with large electron-vibron coupling in the Coulomb blockade regime. We show that when the electron-vibron coupling induces polaron states, the current-voltage characteristic becomes strongly asymmetric because, in one current direction, one of the polaron states blocks the current through the other. This situation occurs when the coupling between the polaron states is smaller than the coupling to the leads. We discuss the relevance of our calculation for experiments on C_{140} molecules.

DOI: 10.1103/PhysRevB.71.155408

PACS number(s): 73.63.Kv, 85.65.+h, 85.35.Gv

I. INTRODUCTION

The possibility of designing molecular junctions that behave as rectifiers was suggested by Aviram and Ratner¹ based on an asymmetric two-level donor molecular system, with one level empty and one filled (an acceptor and a donor level). In one bias direction the levels are tuned closer to resonance, whereas for the reverse bias they are further detuned, giving rise to an asymmetric current-voltage (I - V) characteristic. This scenario has been investigated in molecular systems for a number of years.² The transport properties depend crucially on both the Coulomb interactions and the relaxation of the nuclei during the electron transfer processes. The Coulomb interactions limit the allowed charge configurations, while the electron-vibron coupling determines the overlap between the different configurations as well as provides channels for energy relaxation.

Molecular transistors with strong electron-vibron coupling has recently become an active research area, both experimentally³⁻⁶ and theoretically.⁷⁻¹⁷ Different types of vibrational modes have been observed. In the original work of Park *et al.*³ clear signatures of phonon sidebands were seen in the tunnel spectrum. The size of the individual steps in the I - V curves agreed well with a simple model based on Franck-Condon physics.³ Furthermore, sidebands caused by internal vibration of the molecular systems have also been identified experimentally and, in particular, in a recent experiment by Pasupathy *et al.*⁶ where tunneling through dimerized C_{70} molecules was measured. These authors claimed that a vibrational mode at 11 meV due to the relative motion of the two C_{70} molecules was seen in the experiment.

In this paper, we study theoretically transport through a dimer molecule with a single internal vibration. As a generic model, we include a coupling between the charge on the two parts of the dimer. The electron-vibron coupling thus introduces a possibility of forming polaronic states. Transport in systems with polarons¹⁸ is a well-studied subject and the polaron formation is known to reduce the mobility. In single-electron transistor systems polaronic effects have also been studied theoretically, in particular for single-level systems⁷⁻¹⁵ and only recently for a two-level system.¹⁷ Here we study a similar system but with the important modification that the two levels in addition are coupled by tunneling, in which

case an internal polaron can form. The main point of our study is that when this electron-vibron coupling is sufficiently strong and a polaron state is formed, it may lead to rectification effects and negative differential conductance, depending on how the molecule is situated in the constriction.

The paper is organized as follows. In Sec. II we set up the model describing the dimer and the electron-vibron coupling, in Sec. III we discuss the physical concepts in a semiclassical picture, and in Sec. IV we calculate the transport in the situation where the tunneling rates are smaller than the polaron couplings, whereas Sec. V discusses the situation when the polarons are localized on the time scale set by tunneling to the leads. The crossover between these two regime is studied in Sec. VI and finally Sec. VII discusses the experimental relevance and concludes.

II. MOLECULAR DIMER MODEL

The molecular model that we study (see Fig. 1) is a dimer with two electron sites or, in a different terminology, a “double quantum dot.” For simplicity, we neglect both spin and possible orbital degeneracies in the model. The two sites are coupled by tunneling. Furthermore, due to an electric field across the gap, the internal molecular vibrational mode couples to the charges difference on the two sites. The electric field is produced either by the bias voltage, local charge traps, or image charges created in the leads by the charged molecule. In total our model Hamiltonian for the molecule reads

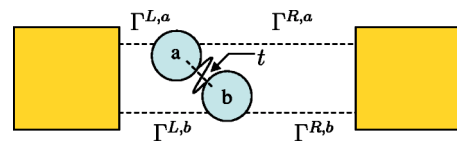


FIG. 1. Dimer model studied in this paper. The two parts of the dimer are represented by single electronic levels a and b connected by a tunneling amplitude t . The intramolecular vibration is illustrated as a spring connecting the two levels. A force acts on the part of the dimer that is occupied by an electron due to an electric field in the gap.

$$H_D = \frac{p^2}{2m} + \frac{1}{2}m\omega^2x^2 + \Delta(n_a - n_b) + eV_g(n_a + n_b) + Un_a n_b - t(c_a^\dagger c_b + c_b^\dagger c_a) + \lambda(n_a - n_b)x. \quad (1)$$

Here c_j^\dagger (c_j) ($j=a,b$) are the electron creation (annihilation) operators, whereas b^\dagger (b) is the vibron creation (annihilation) operator and $n_j=c_j^\dagger c_j$. Furthermore, V_g is the gate voltage which couples to the total charge on the molecule, Δ describes the energy difference between the two sites, and, finally, U the Coulomb repulsion between electrons occupying the two levels. The total Hamiltonian describing the molecule, the leads, and the coupling between them is

$$H = H_D + \sum_{\eta=L,R} (H_\eta + H_{T\eta}), \quad (2)$$

where

$$H_\eta = \sum_k \xi_{k\eta} c_{k\eta}^\dagger c_{k\eta} \quad \eta = L, R, \quad (3)$$

$$H_{T\eta} = \sum_{k,j=a,b} (T_{k\eta,j} c_{k\eta}^\dagger c_j + T_{k\eta,j}^* c_j^\dagger c_{k\eta}). \quad (4)$$

Throughout, we will assume large U and a gate voltage tuned such that the total occupancy is either zero or one. The subspace with zero electrons is, of course, easily diagonalized. With one electron on the dimer, the situation is more complicated. Introducing Pauli matrices for the electronic degree of freedom and the dimensionless parameters (using $\hbar=1$)

$$\alpha = \frac{\lambda^2}{m\omega^2 t}, \quad g = \frac{\lambda^2}{2m\omega^3}, \quad \delta = \frac{\Delta}{\omega}, \quad (5)$$

we are left with the Hamiltonian

$$H_D/\omega = b^\dagger b + \frac{1}{2} + \sqrt{g}\hat{\sigma}_z(b^\dagger + b) - \frac{2g}{\alpha}\hat{\sigma}_x + \delta\hat{\sigma}_z + eV_g, \quad (6)$$

where b and b^\dagger are the usual boson annihilation and creation operators. This Hamiltonian can be solved numerically in a truncated boson Hilbert space, which is done below in order to determine the eigenenergies and the overlap factors between the empty and occupied molecules. At $\alpha=1$ there is a crossover to a regime where the fermion and boson degrees of freedom become strongly correlated due to the formation of polaron states. When the levels are nondegenerate the polaron leads to an increased localization of the electronic wave function. In both cases there is a strong reduction of the effective tunneling amplitude between the two sites, which has consequences for conductance through the molecule.

III. SEMICLASSICAL ANALYSIS

In order to understand the polaron formation, we start by a semiclassical analysis of the spin-boson model. This is done in order to illustrate the physics and will not be used in the actual description described in the following sections. The semiclassical treatment is formally valid when $\omega \ll t_{\text{eff}}$, but in the examples taken below this is not the case, and we

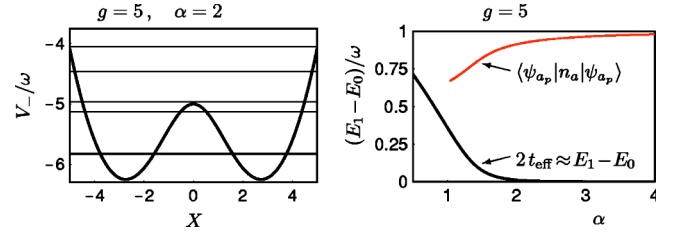


FIG. 2. Left panel: the semiclassical potential for $g=5$ and $\alpha=2$ and the exact eigenvalues (horizontal lines) found by numerical diagonalization of Eq. (6). Note that the two lowest eigenvalues are almost degenerate, corresponding to two polaron states split by a small effective tunneling coupling t_{eff} . The effective coupling is shown in the right panel as a function of α together with the electron population of level a in the polaron state ψ_{a_p} , defined in Eq. (9). The remaining eigenenergies are not degenerate and therefore the corresponding eigenstates are delocalized on the molecule.

instead resort to numerical diagonalization of the Hamiltonian in Eq. (6).

Treating the harmonic oscillator classically, the model can be solved in electronic Hilbert space. The electronic Hamiltonian then becomes

$$H_{De} = \omega \begin{pmatrix} \sqrt{2g}X + \delta & -2g/\alpha \\ -2g/\alpha & -\sqrt{2g}X - \delta \end{pmatrix}, \quad (7)$$

where $X=x/\ell$ and $\ell=\sqrt{1/m\omega}$. For each of the two electronic eigenstates we thus have an effective potential for the oscillator degree of freedom. These Born-Oppenheimer surfaces are

$$\frac{V_{\pm}}{\omega} = \frac{1}{2}X^2 \pm \sqrt{2gX^2 + \frac{4g^2}{\alpha^2} + 2\sqrt{2g}X\delta + \delta^2}. \quad (8)$$

In the electronic ground state V_- there is only one minimum for $\alpha < 1$, whereas for $\alpha > 1$ there are two minima. Thus a bifurcation occurs at $\alpha=1$. In the bifurcated domain, the electronic and bosonic degrees of freedom become highly correlated, because when the oscillator is localized in one of the two minima, the electron wave function is changed accordingly. Thus the physics is similar to that of a small polarons (see Fig. 2). In Fig. 2 we show the bifurcated potential, the exact numerical eigenvalues, and the effective tunneling coupling between the polaron states. From our exact diagonalization we thus find that the difference in energy between the ground state and the first excited state becomes exponentially small in the polaron regime.

In the semiclassical picture, the splitting of the polaron states occurs because of tunneling. The tunneling amplitude is small, because in order to move, it must drag the oscillator displacement with it. Furthermore, a coupling to a dissipative environment will tend to localize the polaron even more, because it couples to displacement coordinate and thus tends to destroy the coherence between the two states,¹⁹ resulting in a small effective tunneling coupling t_{eff} . When the effective coupling becomes very small, the two lowest eigenstates $|\psi_0\rangle$ and $|\psi_1\rangle$ form two polaron states which are approximate eigenstates:

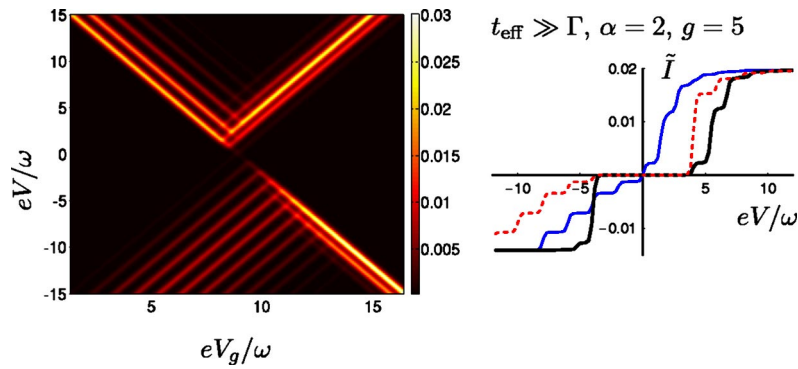


FIG. 3. (Color online) Left panel: contour plot showing the differential conductance for the dimer molecule in the regime Eq. (12) where holds. The parameters are $g=5$, $\alpha=2$, $\Delta=0$, $\Gamma^{Ra}=0$, $\Gamma^{Rb}/\Gamma^{La}=0.04$, $\Gamma^{Lb}/\Gamma^{La}=0.96$, and $T=0.1\omega$. The bias voltage is applied symmetrically, so that $V_L=-V_R=V/2$. Notice the suppression of the differential conductance at low bias voltage which is due to an overlap between the filled and empty states. The right panel shows I - V curves for the same parameters (but $T=0.05\omega$) for $V_g-V_{g0}=0$ (curve without gap at $V=0$), -2ω (dashed curve), and 2ω . Here V_{g0} defines the gate voltage at which the ground states of the two charge states are degenerate.

$$|\psi_{a_p}(b_p)\rangle = (|\psi_0\rangle \pm |\psi_1\rangle)/\sqrt{2}. \quad (9)$$

As long as the splitting in energy is larger than the tunneling broadening of the levels, the polaron formation is not important for the transport other than it influences the Franck-Condon factors and the molecule can still be regarded as one quantum system (see Fig. 3). This situation is analyzed in Sec. IV. However, if the effective tunneling rate t_{eff} is smaller than the tunneling rates to and from the leads, a different physical picture emerges, because the dimer will behave as a “double dot” with weak interdot coupling but strong Coulomb interaction (see Fig. 4). Thus a master equation treatment should take into account that the molecular system has more internal states, which is done in Sec. V. This regime is where the rectification occurs as discussed in detail below.

IV. TRANSPORT PROPERTIES FOR $\Gamma \ll t_{\text{eff}}$

As argued, the transport properties of the dimer transistor depend on the ratio between tunneling rates and internal time scales of the molecule. Let us first assume that all tunneling rates Γ^{Ra} , Γ^{Rb} , Γ^{La} , and Γ^{Lb} are much smaller than t_{eff} . Furthermore, throughout we consider the weak-tunneling limit in the sense that the vibrational degrees of freedom are assumed to relax between tunneling events—i.e., $\omega/Q \gg \Gamma$, where Q is the quality factor of the vibrational mode.¹¹ If this limit is not satisfied, the nonequilibrium vibron distribution should also be determined; however, for the physics discussed here this is not important. Also, the broadening of the vibron sidebands is not included and assumed dominated by the thermal smearing such that $k_B T \gg \omega/Q$. To describe this situation, we now use the master equation approach and only

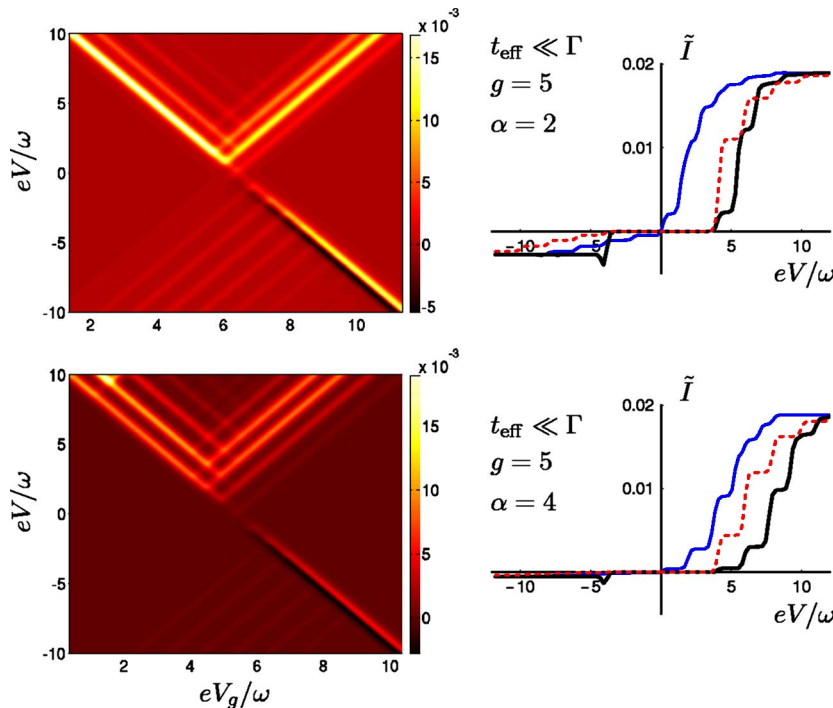


FIG. 4. (Color online) Left panel: contour plots showing the differential conductance for the dimer molecule when Eq. (19) holds, for $\alpha=2$ (top) and $\alpha=4$ (bottom). Other parameters are $g=5$, $\Delta=0$, $\Gamma^{Ra}=0$, $\Gamma^{Rb}/\Gamma^{La}=0.04$, $\Gamma^{Lb}/\Gamma^{La}=0.96$, and $T=0.1\omega$. The bias voltage is applied symmetrically, so that $V_L=-V_R=V/2$. Right panels show corresponding I - V curves for different gate voltages as in Fig. 3 and with $T=0.05\omega$. Note the strong blocking of the current in one direction and the negative differential resistances. For $\alpha=2$ the current in the blocked direction is larger than for $\alpha=4$, because the polaron is less localized on one electron level (see Fig. 2).

the occupations of the different charge states need to be determined by the kinetics. Allowing only two charge states, with occupations P_0 and P_1 , the master equation is

$$-P_1\Gamma_{01} - P_0\Gamma_{10} = 0, \quad (10)$$

together with the normalization condition

$$P_0 + P_1 = 1. \quad (11)$$

Here Γ_{ij} is the tunneling rate from state j to state i . The expression for the current then becomes

$$I = (-e) \frac{\Gamma_{10}^R \Gamma_{01}^L - \Gamma_{01}^R \Gamma_{10}^L}{\Gamma_{10}^R + \Gamma_{10}^L + \Gamma_{01}^R + \Gamma_{01}^L} \quad (\Gamma \ll t_{\text{eff}}). \quad (12)$$

In Eqs. (10) and (12) the tunneling rates are calculated using Fermi's golden rule. When calculating the rates in Eq. (12) we encounter tunneling densities of states of the form $\Gamma^\eta = 2\pi \sum_k |T_{k\eta,j}|^2 \delta(\xi_{k\eta})$ ($\eta=L,R$). The evaluation of the cross terms $\sum_k T_{k\eta,a}^* T_{k\eta,b} T_{k\eta,b} \delta(\xi_{k\eta})$ requires detailed knowledge of the relative phases of the tunneling amplitudes to the two parts of the dimer. Fortunately, a simplification is possible because $T_{k\eta,a}^* T_{k\eta,b} \sim \exp(ikd)$, where d is the distance between the two parts of the dimer and k is the wave number of the lead electrons. Typically, one has $kd \gg 1$ and the cross terms average to zero when summing over k . Thus, no interference effects between the two tunneling paths onto the molecule is expected. With these observations, we obtain

$$\Gamma_{10}^\eta = \sum_{j=a,b} \Gamma^\eta \sum_{i_0, f_1} |\langle f_1 | c_j^\dagger | i_0 \rangle|^2 \frac{e^{-\beta E_{i_0}}}{Z_0} n_\eta(E_{f_1} - E_{i_0}) \quad (13)$$

and

$$\Gamma_{01}^\eta = \sum_{j=a,b} \Gamma^\eta \sum_{i_1, f_0} |\langle f_0 | c_j | i_1 \rangle|^2 \frac{e^{-\beta E_{i_1}}}{Z_1} [1 - n_\eta(E_{i_1} - E_{f_0})]. \quad (14)$$

Here, $|i_0\rangle$, $|i_1\rangle$ ($|f_0\rangle$, $|f_1\rangle$) denote initial (final) states of the empty (0) and filled (1) dimer and

$$n_\eta(E) = 1 / \{\exp[(E - eV_\eta)/k_B T] + 1\} \quad (15)$$

are the Fermi functions in the lead η with applied voltages V_η . Finally, E_{i_n} and E_{f_n} are the total dimer energies for the initial and final states with n electrons and Z_0 and Z_1 the corresponding partition functions.

Because we are interested in the asymmetric situation, we study the situation where one electrode couples stronger than the other to the molecule, $\Gamma^R \ll \Gamma^L$. Furthermore, we also allow for a skewed configuration as in Fig. 1, and in this geometry, we have $\Gamma^{Ra} < \Gamma^{Rb}$ and $\Gamma^{La} > \Gamma^{Lb}$. In Fig. 3, we show examples of the differential conductance in the V - V_g plane in the situation where the intramolecular coupling between polaron states is strong—i.e., when $\Gamma \ll t_{\text{eff}}$ and Eq. (12) applies. Furthermore, the bias voltage is applied symmetrically, so that $V_L = -V_R = V/2$.

V. TRANSPORT PROPERTIES FOR $\Gamma \gg t_{\text{eff}}$

In the opposite case $\Gamma \gg t_{\text{eff}}$, the situation is very different. In this case, an electron that tunnels onto level a does not

resolve the tunneling splitting of the two polaron states and the molecule no longer relaxes between tunneling and therefore the two polaron states can be considered as decoupled. In this case, we must treat the filled molecule as a quantum system having *more* possible states, since it can be occupied in one of the two polaron states, from now on denoted by a_p and b_p . Furthermore, the molecule may be occupied in one of the delocalized states (see Fig. 2).

Moreover, we consider the hierarchy of energies $\omega > k_B T > \omega/Q > \Gamma > t_{\text{eff}}$. The last two inequalities imply that between tunnelings the molecule relaxes to a thermal distribution within each polaron subspace. Since the current drives the occupancies of the two polaron states out of equilibrium, we need to determine the distribution functions of the two polaron states P_{a_p} and P_{b_p} , respectively. If the molecule is occupied in a delocalized state, it is in either polaron state with equal probability. The new set of master equations thus reads (with $\tau = a_p$ or $\tau = b_p$)

$$-P_\tau \Gamma_{01}^\tau - P_0 \Gamma_{10}^\tau = 0, \quad (16a)$$

$$-P_0 \sum_\tau \Gamma_{01}^\tau - \sum_\tau P_\tau \Gamma_{10}^\tau = 0, \quad (16b)$$

together with the condition

$$P_0 + \sum_\tau P_\tau = 1. \quad (16c)$$

The tunneling rates in Eq. (16) have contributions from both leads:

$$\Gamma^\tau = \sum_{\eta=L,R} \Gamma^{\eta,\tau}. \quad (16d)$$

The tunneling rate for tunneling from lead η into a_p is (again the oscillating cross terms are ignored)

$$\Gamma_{10}^{\eta,a_p} = \sum_{j=a,b} \Gamma^\eta \sum_{i_0, f_1^{a_p}} |\langle f_1^{a_p} | c_j^\dagger | i_0 \rangle|^2 \frac{e^{-\beta E_{i_0}}}{Z_0} n_\eta(E_{f_1^{a_p}} - E_{i_0}), \quad (17)$$

and similarly for tunneling into the polaron states b_p . Here $|f_1^{a_p}\rangle$ and $|f_1^{b_p}\rangle$ mean the polaron states in Eq. (9) if they are degenerate—i.e., $(|f_1^{(1)}\rangle \pm |f_1^{(2)}\rangle) / \sqrt{2}$, where $|f_1^{(i)}\rangle$, $i=1,2$, are the two degenerate states (meaning that eigenenergies differ by less than Γ). For the nondegenerate states, $|f_1^{a_p}\rangle = |f_1^{b_p}\rangle = |f_1\rangle$, implying that the system ends up in either polaron state with equal probability.

For the tunneling-out processes the rates are

$$\Gamma_{01}^{\eta,a_p} = \sum_{j=a,b} \Gamma^\eta \sum_{i_1^{a_p}, f_0} |\langle f_0 | c_j | i_1^{a_p} \rangle|^2 \frac{e^{-\beta E_{i_1^{a_p}}}}{Z_1^{a_p}} [1 - n_\eta(E_{i_1^{a_p}} - E_{f_0})], \quad (18)$$

where the initial polaron states are defined in the same way as above. Similar expression holds for tunneling out of the polaron state b_p . Thus, treating the dimer as separate polaron states, we find a different expression for the current:

$$I = (-e) \frac{\sum_{\tau} [\Gamma_{10}^R \Gamma_{01}^{L\tau} - \Gamma_{10}^L \Gamma_{01}^{R\tau}] / \Gamma_{01}^{\tau}}{1 + \sum_{\tau} (\Gamma_{10}^{\tau} / \Gamma_{01}^{\tau})} \quad (\Gamma \gg t_{\text{eff}}). \quad (19)$$

In Fig. 4 we show the results in the case where $\Gamma \gg t_{\text{eff}}$ and Eq. (19) holds. The I - V characteristics are seen to be strongly asymmetric even though the bias is applied in a symmetric way—i.e., $V_L = -V_R = V/2$. The reason for the asymmetry is that the polaron state, which is weakly coupled to the right lead, can block current through the other, more strongly coupled state. However, this blockade only happens in one current direction—namely, when the electrons run toward the weakly coupled electrode.

VI. CROSSOVER REGIME: GENERALIZED MASTER EQUATION

In the regime where Γ and t_{eff} are of the same order, we cannot use any of the two approaches above, because when two states in the molecular system are degenerate or closer than Γ in energy, the current through the system has to be described as one coherent process. This is in general a difficult problem. However, in the limit of large bias voltage a generalized master equations^{20–23} has been developed. To study how the asymmetry of the large bias conductance, we here adopt this method. The large bias assumption implies that the voltage must be large compared to the temperature and the (effective) tunneling couplings as well molecular energies. The assumption of large bias leads to the set of Markovian master equations for the density matrix.^{20–23} Thus at large bias there is no correlation between individual tunneling events, but still the transfer of electrons is described coherently. The generalized master equation approach can, in fact, describe the crossover we discuss here, because the blocking effect found in Sec. V does not depend on time correlations between tunnel events, but on how strongly a single electron is localized on the molecule during tunneling.

Furthermore, in order to simplify the problem we consider only the two lowest states which correspond to the two polaron states located to the left or to the right with some effective coupling t_{eff} . The generalized master equations are then a modification of those developed in Ref. 21 for a double-dot system, because here we allow for in and out tunnelings on both dots. For the case when the electron current is from left to right (i.e., $V < 0$), we have

$$\partial_t \rho_{aa} = \Gamma^{La_p} \rho_0 - \Gamma^{Ra_p} \rho_{aa} + it_{\text{eff}}(\rho_{ba} - \rho_{ab}), \quad (20a)$$

$$\partial_t \rho_{bb} = \Gamma^{Lb_p} \rho_0 - \Gamma^{Rb_p} \rho_{bb} - it_{\text{eff}}(\rho_{ba} - \rho_{ab}), \quad (20b)$$

$$\partial_t \rho_{ab} = \left[-\frac{1}{2}(\Gamma^{Ra_p} + \Gamma^{Rb_p}) + i\Delta \right] \rho_{ab} + it_{\text{eff}}(\rho_{bb} - \rho_{aa}), \quad (20c)$$

$$\partial_t \rho_{ba} = \left[-\frac{1}{2}(\Gamma^{Ra_p} + \Gamma^{Rb_p}) - i\Delta \right] \rho_{ba} - it_{\text{eff}}(\rho_{bb} - \rho_{aa}). \quad (20d)$$

The stationary solution for ρ is found by setting $\partial_t \rho_{ij} = 0$ and the current is then $I = (-e)(\rho_{aa} \Gamma^{Ra_p} + \rho_{bb} \Gamma^{Rb_p})$, which becomes, for $V < 0$,

$$I_{V < 0} = \frac{(-e) \Gamma^L \Gamma^R (\chi_R \Gamma^R + \Gamma^{Ra_p} \Gamma^{Rb_p} / \Gamma^R)}{(\Gamma^R + 2\Gamma^L) \chi_R \Gamma^R + \Gamma^{Ra_p} \Gamma^{Rb_p} (1 + \Gamma^{La_p} / \Gamma^{Ra_p} + \Gamma^{Lb_p} / \Gamma^{Rb_p})}, \quad (21)$$

where

$$\Gamma^R = \Gamma^{Ra_p} + \Gamma^{Rb_p}, \quad \Gamma^L = \Gamma^{La_p} + \Gamma^{Lb_p}, \quad (22)$$

and where

$$\chi_R = \frac{4t_{\text{eff}}^2}{4\Delta^2 + (\Gamma^R)^2} \quad (23)$$

contains all the t_{eff} and Δ dependences. When χ_R is large, the current reduces to the incoherent result of a dot with a doubly degenerate level:

$$I_{V < 0} = \frac{(-e) \Gamma^L \Gamma^R}{\Gamma^R + 2\Gamma^L}. \quad (24)$$

In the opposite limit of small χ_R the time an electron spends on the dimer is too short for hopping between the sites to occur, and the current reduces to

$$I_{V < 0} = \frac{(-e) \Gamma^L}{1 + \Gamma^{La_p} / \Gamma^{Ra_p} + \Gamma^{Lb_p} / \Gamma^{Rb_p}}, \quad (25)$$

which is also the large V limit of Eq. (19) or the sequential tunneling limit of a double-dot system in the absence of interdot tunneling.

The current for positive voltage is easily found from Eq. (21) by interchanging left and right, $L \leftrightarrow R$.

Let us now focus on the limit considered in the examples in the previous two sections—namely, $(\Gamma^R, t_{\text{eff}}) \ll \Gamma^L$ and $(\Gamma^{Ra}, t_{\text{eff}}) \ll \Gamma^{Rb}$ —and in these limits we find the following ratio between the currents for the two bias polarizations:

$$\left| \frac{I_{V < 0}}{I_{V > 0}} \right| = \frac{\Gamma^{Ra_p} / \Gamma^R + \chi_R}{\Gamma^{La_p} / \Gamma^L + 2\chi_R}. \quad (26)$$

From this expression it is evident that degree of rectification is limited by the smallest tunneling-out rate through the right junction, Γ^{Ra_p} , or the the interpolaron tunneling coupling, t_{eff} , through the parameter χ_R in Eq. (23). Equation (26) also shows that when asymmetry is limited by χ_R —i.e., when $\Gamma^{Ra_p} / \Gamma^R \ll \chi_R$ —increasing Δ in fact enhances the rectification, because a finite Δ suppresses tunneling between the two sites.

VII. DISCUSSION AND SUMMARY

Last, we discuss the relevance for the experimental system in Ref. 6, where a single-electron transistor setup was made with single C_{140} molecules as the active element. Of course, our two-level model cannot fully describe the real molecule; nevertheless, a comparison is interesting. Signatures of a 11-meV intramolecular vibrational mode were observed in Ref. 6 and the coupling parameter g was estimated to be between 1 and 5.²⁴ If the polaron physics discussed here should have relevance for this or similar dimer systems,

we must have $\alpha \geq 2$ or, correspondingly, $t \sim 50$ meV, which is not unrealistic. In fact, rectification effects very similar to those predicted in the present paper have indeed been seen in some C_{140} devices.²⁵

In conclusion, we have studied molecular system with an internal vibrational mode coupled to the charge difference between two hybridized molecular levels giving rise to polaron formation. The polaron has distinct consequences for the transport properties, which we have calculated using different master equation approaches. First, we analyzed the case when the internal hybridization between polarons is larger than tunneling rates to the leads. This gives more or less symmetric I - V characteristics, but with a number of vibron sidebands. Second, we studied the case when the two polarons are weakly coupled and the tunneling rates to the leads dominate the kinetics. In this case, another set of master equation was needed and highly asymmetric I - V characteristics are predicted. Finally, we have analyzed the crossover

regime by a generalized master equation capable of describing the coherent tunneling, but only for large bias voltages.

The rectification mechanism suggested in this paper should be experimentally observable. Generally, the current-voltage characteristics of complex molecular transistors with strong coupling between charge and vibrational degrees of freedom is a promising tool for studying the details of such devices.

ACKNOWLEDGMENTS

We thank P. McEuen, J. Park, and A. Pasupathy for discussions on the experiments and T. Novotny and M. Wegewijs for discussions and comments on the manuscript. The work was supported by the Danish Natural Science Foundation and the European Commission through project FP6-003673 CANEL of the IST Priority.

-
- ¹A. Aviram and M. A. Ratner, *Chem. Phys. Lett.* **29**, 277 (1974).
²R. M. Metzger, *J. Am. Chem. Soc.* **103**, 3803 (2003).
³H. Park, J. Park, A. K. L. Lim, E. H. Anderson, A. P. Alivisatos, and P. L. McEuen, *Nature (London)* **407**, 57 (2000).
⁴S. Kubatkin, A. Danilov, M. Hjort, J. Cornil, J. Bredas, N. Stuhr-Hansen, P. Hedegård, and Thomas Bjørnholm, *Nature (London)* **425**, 698 (2003).
⁵L. H. Yu and D. Natelson, *Nano Lett.* **4**, 79 (2004); L. H. Yu, Z. K. Keana, J. W. Ciszek, L. Cheng, M. P. Stewart, J. M. Tour, and D. Natelson, *Phys. Rev. Lett.* **93** 266802 (2004).
⁶A. N. Pasupathy, J. Park, C. Chang, A. V. Soldatov, S. Lebedkin, R. C. Bialczak, J. E. Grose, L. A. K. Donev, J. P. Sethna, D. C. Ralph, and P. L. McEuen, cond-mat/0311150 (unpublished).
⁷N. S. Wingreen, K. W. Jacobsen, and J. W. Wilkins, *Phys. Rev. B* **40**, 11834 (1989).
⁸D. Boese and H. Schoeller, *Europhys. Lett.* **54**, 668 (2001).
⁹U. Lundin and R. H. McKenzie, *Phys. Rev. B* **66**, 075303 (2002).
¹⁰K. Flensberg, *Phys. Rev. B* **68**, 205323 (2003).
¹¹S. Braig and K. Flensberg, *Phys. Rev. B* **68**, 205324 (2003).
¹²K. D. McCarthy, N. Prokof'ev, and M. T. Tuominen, *Phys. Rev. B* **67**, 245415 (2003).
¹³A. S. Alexandrov, A. M. Bratkovsky, and R. S. Williams, *Phys. Rev. B* **67**, 075301 (2003); A. S. Alexandrov and A. M. Bratkovsky, *ibid.* **67**, 235312 (2003).
¹⁴A. Mitra, I. Aleiner, and A. J. Millis, *Phys. Rev. B* **69**, 245302 (2004).
¹⁵M. Galperin, M. A. Ratner, and A. Nitzan, *Nano Lett.* **4**, 1605 (2004).
¹⁶H. Ness, S. A. Shevlin, and A. J. Fisher, *Phys. Rev. B* **63**, 125422 (2001).
¹⁷M. Wegewijs *et al.*, in *Introducing Molecular Electronics*, edited by G. Cuniberti *et al.* (Springer, Berlin, in press).
¹⁸T. Holstein, *Ann. Phys. (N.Y.)* **8**, 343 (1959).
¹⁹A. J. Leggett, *Rev. Mod. Phys.* **59**, 1 (1987).
²⁰S. A. Gurvitz and Y. S. Prager, *Phys. Rev. B* **53**, 15932 (1996).
²¹T. H. Stoof and Yu. V. Nazarov, *Phys. Rev. B* **53**, 1050 (1996).
²²S. A. Gurvitz, *Phys. Rev. B* **57**, 6602 (1998).
²³M. R. Wegewijs and Y. V. Nazarov, *Phys. Rev. B* **60**, 14318 (1999).
²⁴In extracting g , one should, however, be aware that the peak height distribution is not Poissonian.
²⁵A. N. Pasupathy *et al.* (Ref. 6); (private communication).